Non-Invasive Microwave Imaging via Linear Antenna Array

Daniel A. Edwards[1]
[1]Department of Electrical and Computer Engineering, University of Alabama, Tuscaloosa, AL 35487, USA

ABSTRACT The existence of foreign objects inside of foodstuffs and poor-quality food objects in general is a common issue in the food industry. Through the use of a Microwave Imaging system, it is possible to scan and reconstruct a digital image of any object(s) scanned. This report covers the experimentation of a converted circular antenna array software to a linear system. With the use of a Vector Network Analyzer, multiple scans of an object are taken as it moves through the antennas on an automatic conveyor belt. Then, these scans are loaded into a MATLAB Script that utilizes the MERIT functions and beamforming to convert the s-parameter wave data into a 2D colormap image. The goals of this project were to successfully reconstruct the image of a Peanut Butter Jar, the location of an impurity inside a Peanut Butter Jar, and to also reconstruct various other objects passed through the antennas. This would help to solve the issue of foreign objects and misshapen food objects in the food industry, as a cheap and easy solution that adapts to any inline conveying belt inside a factory. Through the techniques in this report, object reconstruction and impurity detection were proven possible with some inaccuracy regarding object width in the Y dimension, and impurity location in the X dimension due to wave symmetry.

INDEX TERMS Beamforming, Linear Antenna Array, MATLAB, MERIT, Microwave Imaging, Permittivity, S-parameter, Vector Network Analyzer

I. INTRODUCTION

Determining the location of impurities and foreign objects inside foods as well as misshapen or damaged goods have always been a common issue within the food industry. A small shard of metal, glass, or even plastic inside a jar of peanut butter has the potential to stay hidden during food preparation until it causes harm to the consumer. One possible candidate that can prevent these issues is the use of Electromagnetic (EM) sensors. Specifically, Microwave Imaging (MWI) can help shape and therefore detect food quality and possible contaminants in a fast and non-damaging way. An example of this proving successful is in the article "Non-invasive Inline Food Inspection via Microwave Imaging Technology" and its solution method determined that Introducing a Linear system into the current food industry is the most desired format as inline food processing is most commonly used for packaged goods [1]. This means the MWI process must take place as an object passes through the antennas on an automatic conveying belt. This project's scope is the same but instead with use of two Coplanar Vivaldi (CV) antennas rather than Horn Antennas. This report also focuses on the reconstruction of the food object as a whole, rather than just the location of any impurities within the food object.

The MATLAB script was adapted from a Circular Antenna Array system developed for Microwave imaging of a watermelon's maturity [2]. This software will be mainly powered by the open-source MERIT toolbox available on GitHub [3]. MERIT was originally designed to detect Inhomogeneous Breast Phantoms but was further developed for general MWI [4]. The previous circular antenna array system uses this toolbox as well and focuses on the use of the Delay and Sum beamforming algorithm (DAS). Beamforming is a signal processing technique that focuses EM signals to designated channels for directional transmission. MERIT offers other beamforming algorithms, however, which are discussed in this report. These are defined as theoretically improved DAS algorithms known as "Modified Delay and Sum" [6] and "Delay Multiply and Sum" [5].

II. DATA CAPTURE

As data capture is the first part of the MWI process, it's important to discuss the tools used to gather the Scattering Parameter Files necessary for image construction. The Vector Network Analyzer (VNA) used was an Agilent Technologies PNA Network Analyzer, model number E8364C, that ranges from 10MHz-50GHz. This VNA was connected to two CV antennas originally fabricated and used in the circular antenna array system previously mentioned. These antennas "exhibit wide bandwidth, high gain and efficiency and simple fabrication [2]." The antennas were slid into a wooden stand overlooking an Automatic Conveying Belt constructed specifically for this project. An image overlooking the conveyor setup is shown in *Figure 1*. The conveyor belt is powered by two STEPPERONLINE Stepper Motors, model number 17HS19-2004S1.

The entire data capture process is fairly automatic thanks to the Visual Studio code and Arduino device provided by Dr. Jeong and his previous students. This Automatic Conveyor Software allows the user to input specific parameters that control the conveyor behavior. This program includes a continuous mode and an interval mode, which is what was used during the entirety of this project. The interval mode is designed to allow for the user to select the total number of increments the conveyor shifts, how far it shifts during each increment, and the filename of the scans it takes after each increment shift.

This means that after the conveyor has completed its total increments, all that's left is to connect to the VNA on the Lab Room's network and save the Scattering Parameter Files (S2P) to your device.
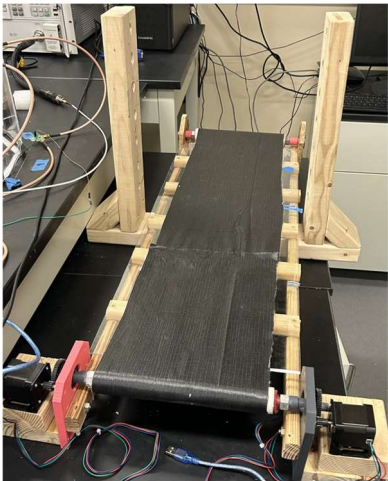

Figure 1. Automatic Conveyor and Antenna Posts

For the duration of the testing process, it was important that a standardized imaging domain was determined. For this project, the object will begin on the far negative side of an X axis and move along the conveyor towards the positive direction, passing over the origin. The Antennas are located at the origin of the X axis and on the positive and negative edges of the Y axis in the imaging domain. This leaves the Z axis representing the height of the Object and Antennas relative to the Conveyor Belt. An image representing the X-Y plane is shown in *Figure 2*.
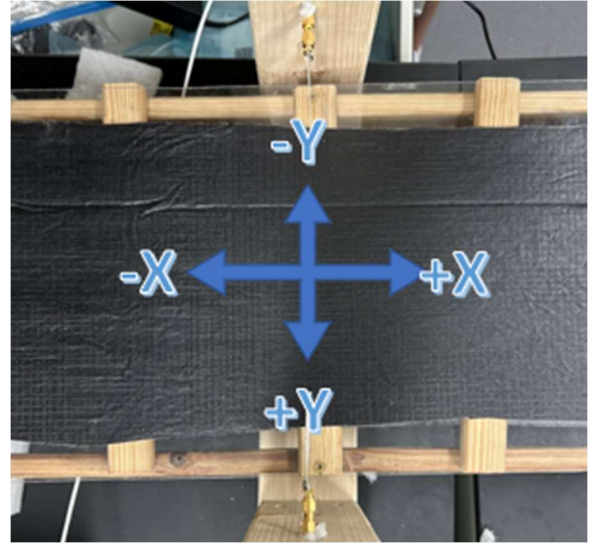

Figure 2. X-Y Axis Representation

Various starting positions and increments were experimented with throughout testing, and it was determined that starting 10 centimeters in the negative X direction with increments of 2-millimeter changes towards the positive X direction (dx) were the most efficient in the image reconstruction process. It was realized that starting 15 centimeters away caused currently undiagnosed issues within the imaging process. Using 2mm increments allows for accurate and detailed imaging of any object sent through. Since the object needs to pass through and equally past the antenna array, this meant each scanning process needed to move and scan 100 times. On average, each scanning process takes 3 minutes and 38 seconds according to the Automatic Conveyor software.

III. RECONSTRUCTION PROCESS

The Microwave Radar-based Imaging Toolbox (MERIT) [3] is the driving MATLAB code that allows for image reconstruction. MERIT uses beamforming algorithms to exploit the dielectric contrast in the materials of an object being scanned and a separate scan designated as the reference scan, where normal conditions are set. If the desire is to scan and reconstruct an entire object, then the reference scan is that of Air, with the food object being the object scan. If the desire is to locate an impurity or foreign object, then a normal scan of a perfect food object is used as reference. The exploitation of permittivity of the object (C) and the reference (ε_b) result in the variation of electric contrast between scans ($\Delta\chi$).

$$\Delta\chi = (\varepsilon_c - \varepsilon_b)/\varepsilon_b \qquad (1)$$

In order to achieve accurate images, the delays of wave propagation from the Transmitting Antenna to the Receiving Antenna must be calculated. MERIT makes this simple using its built in "get_delays" function. This function estimates the propagation path based on the Euclidean distance between the antennas [3]. The formula representing this is shown below, where the time delay (T_{mn}) is the time delay of the signal from the transmitting antenna (m) to the receiving antenna (n) and v being the velocity of the EM wave.

$$T_{mn}(p) = \frac{1}{v}\{ \sqrt{(x_m - x)^2 + (y_m - y)^2 + (z_m - z)^2} + \sqrt{(x_n - x)^2 + (y_n - y)^2 + (z_n - z)^2}\} \qquad (2)$$

The dielectric property of the imaging domain, or relative permittivity (ε_r) is needed for this process to work. This is the most varying component of the image reconstruction process as it needs constant adjustment to find the right value, depending on the object, to resolve a clear image.

With all this in mind, there are five major components needed to integrate MERIT. These are the Scan Data, Relative Permittivity, Channel Names, Frequencies, and Antenna Locations.

A. RELATIVE PERMITTIVITY
Relative permittivity can be altered throughout the imaging process, and a good range is between 1-10 for most objects.

B. ANTENNA LOCATIONS
Antenna Locations is needed due to the original use of MERIT being for a Circular Antenna Array system, meaning there were multiple sets of Transmitting and Receiving Antennas. In our case, we can create synthetic antenna arrays with the scans of varying object locations along the Conveying Belt. Shown in *Figure 3*, this allows us to take scans of the object from all possible angles as it moves through the array. *Figure 3a* represents the reality of one array in green as the object moves forward, and *Figure 3b* represents the synthetic layout, being that the scan taken first as the object is farthest left, represents the right furthest antenna array in the synthetic system. As the object moves over and past the origin, the scans will represent the antennas moving in the opposite direction. With the known starting positions, total number of scans, and increment lengths (dx), we can generate the (x,y,z) coordinates of our synthetic arrays in MATLAB.
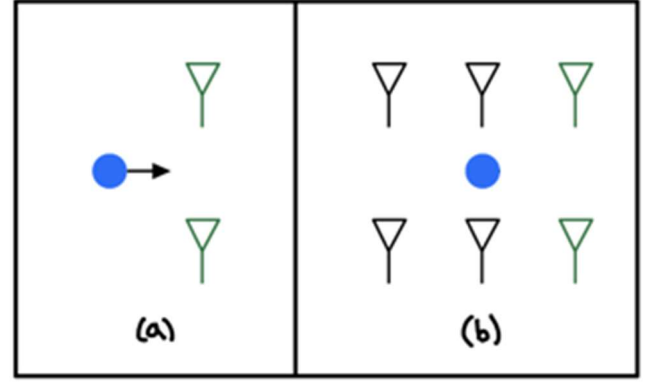

Figure 3: Physical Array vs Synthetic Array

The synthetic antenna locations (red asterisks along X axis at Z level of -0.5) and respective imaging domain can be seen below in *Figure 4,* which also shows a figurative object and its direction of motion.
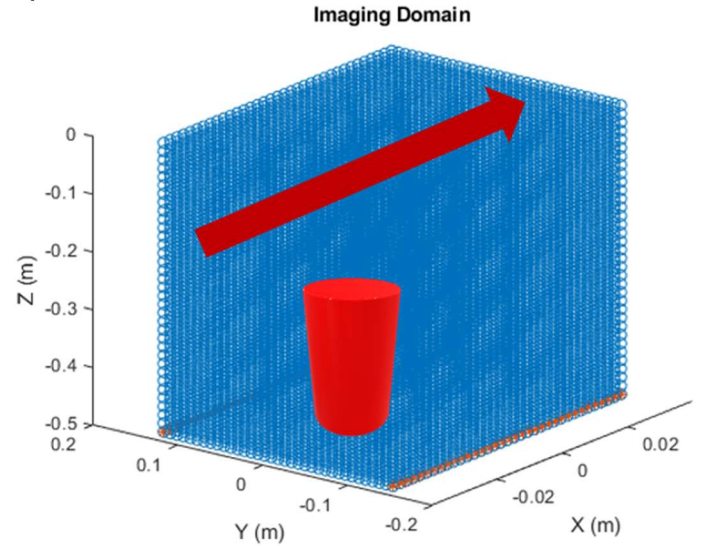

Figure 4. Imaging Domain and Antenna Locations

The antennas are located at a height (or z axis location) of -0.5 meters. Since we are only constructing a 2D image of the object, we will take our visualization slice out of the Z axis. Therefore, we can ignore and potential height calculations, as long as it is confirmed the desired material being scanned is located between the linear antenna arrays. The reason the antennas are located in the negative direction of the Z axis is the original dimensions of X and Y were chosen while only focusing on the 2D dimensions, and for continuity's sake were unchanged during the testing process.

C. CHANNEL NAMES
The channel names are also needed. These tell MERIT the order in which the scans were taken and assign the locations of our antennas to specific sparameter wave data. This is also calculated in MATLAB, based on the total number of scans. *Figure 5* shows the Channel naming process based on a scan set of 100 scans, resulting in

3

naming of 200 antennas. The red arrow representing the object axis of motion, and the blue arrows representing increasing numerical channel names.
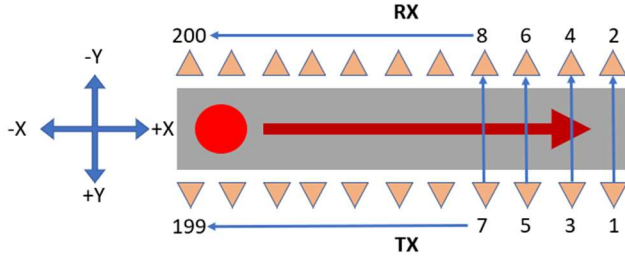

Figure 5. Channel Naming Format

D. SCAN DATA

The last thing needed for image construction is the subtraction scan data. This is the resulting object scan data after simple subtraction of the reference scan data from it. This is done so mainly for artefact detection, removing any scan data involving the surrounding material. It also proves beneficial with general object detection in case there is any stray response with the original air scan. This again is also done in MATLAB and the resulting wave data is normalized using the built in MATLAB function. The normalization function is a heuristic scaling of the wave data to give a greater weight to those signals that more closely resemble the desired case of equal energy [4]. This centers the skewness of our EM response allowing for more details to come forward visibly, but also intensify the response of the stronger responses. An example of this subtraction and normalization can be seen in the results section with *Figure 9b*.

E. FREQUENCIES

This project currently focuses on the use of the S21 parameters of the captured wave data, or bistatic data, calibrated for 2-8GHz. The bandwidth is shown at the top of each reconstructed image in the results section. These frequencies were chosen due to their high response rate with the object as well as being what the CV antennas were designed to be used with.

Once the four major variables needed for MERIT have been generated, we can run the "get_delays" function and then the beamforming function to visualize the image. MERIT offers three major beamforming algorithms. These include Delay and Sum (DAS), Delay Multiply and Sum (DMAS), and Modified Delay and Sum (MDAS). DAS was first used to reconstruct images multistatically, by synthetically focusing signals from each channel and then summing them. The energy of the summed signal at each point is used to reconstruct an energy profile of the imaging domain [3]. DMAS extends DAS by pairwise multiplying

the signals prior to summation and after propagation path compensation. This rewards high coherency (another term for dielectric contrast) and minimizing clutter in the image [5]. MDAS modifies DAS by weighting each point in the imaging domain by a Coherence factor, which is calculated as a ratio of the total energy of the summed signals to the sum of the energy of the input signals [6]. This should reward points with high coherence and inversely lower the response of low coherent points, but throughout testing, MDAS gave poor results and was ignored for the duration of image reconstruction process. For the basic DAS algorithm, the intensity (I_p) of the reconstructed image at each point can be written as

$$I_p(x,y,z) = \int_0^\tau \{\sum_{i=1}^M w_i(x,y,z) * rx_i[t - T_i(x,y,z)]\}^2 \, dt \qquad (3)$$

Where the integration window τ, determined by pulse width, is set to be 50% longer than the input pulse width for this study. The location-dependent weight calculated during preprocessing is denoted as w_i, and rx_i is the received signal. M is the total number of channels, calculated previously, and T_i is the time delay for each channel, calculated in equation 2 [2].

IV. RESULTS

The main bulk of testing can be broken up into three categories. Peanut Butter Jar reconstruction, Varying Object Reconstruction, and Peanut Butter Jar Impurity detection. The first set of results focused on will be the process of constructing a 2D image of a jar of Peanut Butter. The conveying belt setup can be seen in *Figure 6*. This has the jar of peanut butter placed 10cm in the negative X direction and directly in the center of the Y axis.
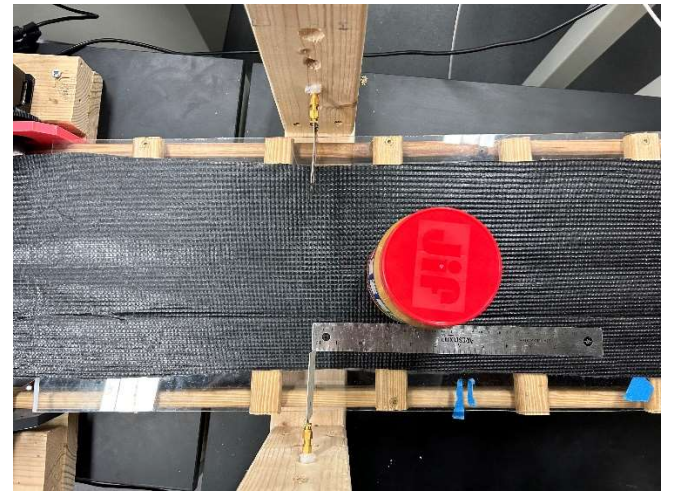

Figure 6. Starting position of Peanut Butter on Conveying Belt

The Automatic Conveyor program was set to take 100 total scans at 2mm intervals, with the peanut butter ending up 10cm in the positive X direction. The antennas were

4

positioned approximately 9.5 cm off of the base stand and 19.5cm apart, ensuring they would be scanning the full width of the peanut butter jar and none of the air space at the top of the jar, shown in *Figure 7*.

Figure 7. Antenna Height to Peanut Butter

The resulting scans were processed through MATLAB and run through a loop testing for permittivity values of 1-10 in increments of 0.1. All results were processed this way and the most accurate images were selected and permittivity values noted. *Figure 8* shows the most accurate 2D image created using the DAS beamforming algorithm, using a high-resolution imaging domain of 55x55 points. The scan data of Air was also subtracted from the Peanut Butter scan data. The black dashed circle represents the actual shape expected of the Peanut Butter, determined by its measured diameter of 98mm.

   As you can see, in the X dimension, the shape has accurate length. The Y dimension seems to be incorrect as it displays a thinner object than what was actually scanned. Based on the results it seems the most accurate permittivity value for scanning the jar of peanut butter is 1.6, the Bandwidth was left at 6GHz as reducing this only slightly sharpened or blurred the image depending on the change.
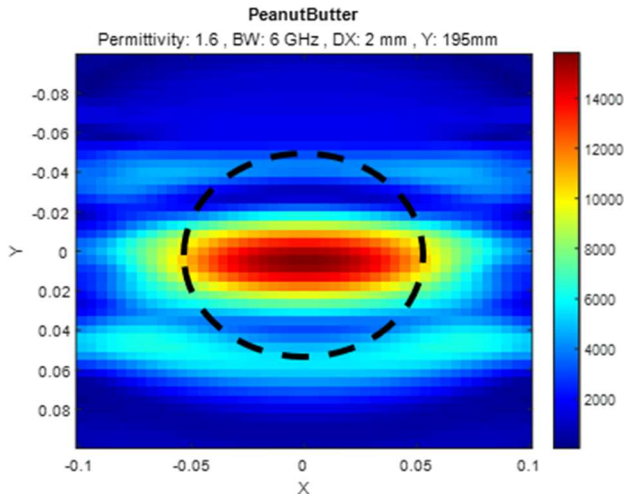

Figure 8. DAS High Resolution PB Construction

The same object was scanned at a later date with the exact same setup and Object, except the antennas were positioned slightly farther apart and the object had impurities placed inside and removed multiple times, likely

resulting in a misshapen and not perfect interior. The distance between the antennas was now 20cm apart. The same permittivity value was chosen, and the result is shown below in *Figure 9a*. The following *Figure 9b* shows the example frequency response plot of the reference air scan in blue and the object scan in red, with the result normalized at the origin in yellow.
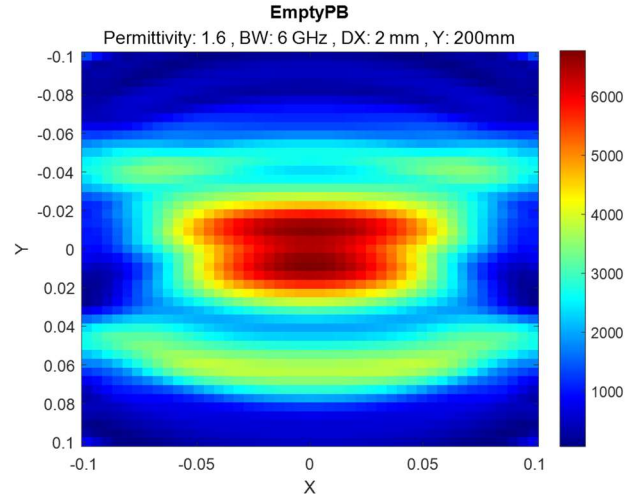

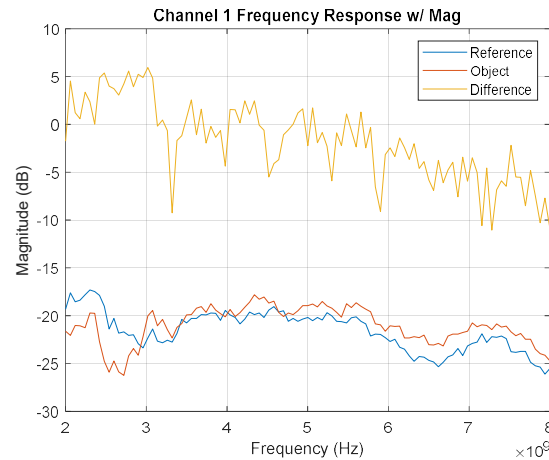*Figure 9a. PB with 200mm Y Dimension*

Figure 9b. PB with 200mm Y Dimension

The thickness of the object has increased in regard to the Y dimension but is still not entirely accurate. The elliptical shape is also not perfect, which usually is due to the permittivity value selected not being ideal. Adjusting the permittivity to 2.3 allows for the elliptical shape to return along with a revised thickness, shown in *Figure 10*. This is likely due to the fact that an increased Y dimension means more air space between the antenna and peanut butter, requiring a different relative permittivity for the new imaging domain. These scans were also processed in the DMAS beamformer but gave similar results with slightly less noise surrounding the main contrast in the center of the image. It should be noted that due to the multiplication of signals before and after summation, DMAS takes much

longer than its MDAS and DAS counterparts. Generating a Medium Resolution (35x35) image takes approximately 8 minutes with 100 scans. Jumping to 150 scans increases this time to ~17 minutes.
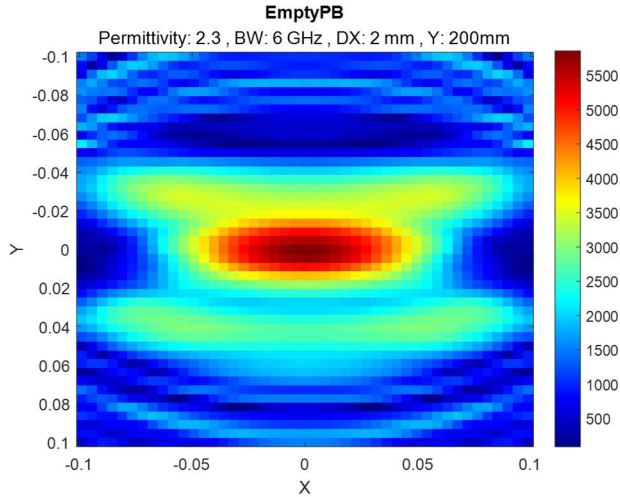

Figure 10. PB using DAS with Permittivity 2.3

Next, the image reconstruction of other objects was conducted. A cylinder of uniform matter (between the antennas) with a diameter of 2.2cm was placed in the imaging domain and scanned in a similar process as the Peanut Butter, beginning in the origin of the Y axis and -10cm in the X axis. An image of this cylinder is shown in *Figure 11* below.
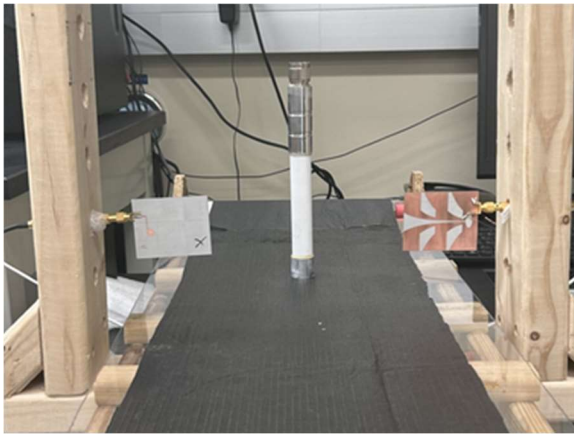

Figure 11. Cylinder of Uniform White Matter

The image construction results are shown below, with the most accurate permittivity value found being 1.8, and the distance between the antennas being adjusted to 16cm apart. In this reconstruction instance, it can be seen that the Y dimension is more accurate, but this might be coincidence. In any case it is noticeable that the thickness of the Y dimension is less than the Peanut Butter counterpart. The X dimension contrast is extremely stretched; however, the strongest response does seem to be much closer to the desired length, with the lighter contrast being due to wave reflections about the object. DMAS was

again tested with the Matter Object scans and produced similar results, however reducing noise and excess symmetry in the Y dimensions due to lower contrast.
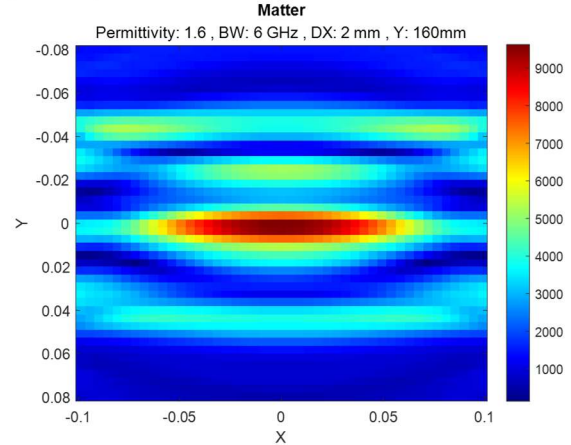

Figure 12. DAS of Matter Cylinder at Origin

Next, scan data was taken of the same object shifted in the negative Y dimension by ~3cm as shown in *Figure 13*. The same reconstruction process was done and using the same permittivity value *Figure 14* shows the resulting image created.
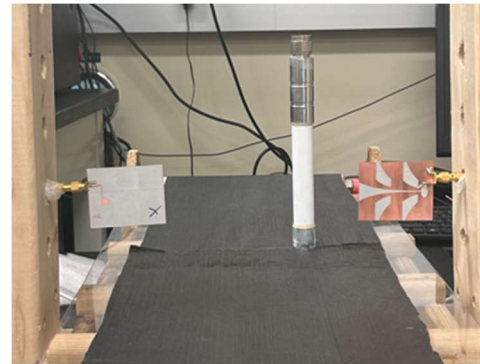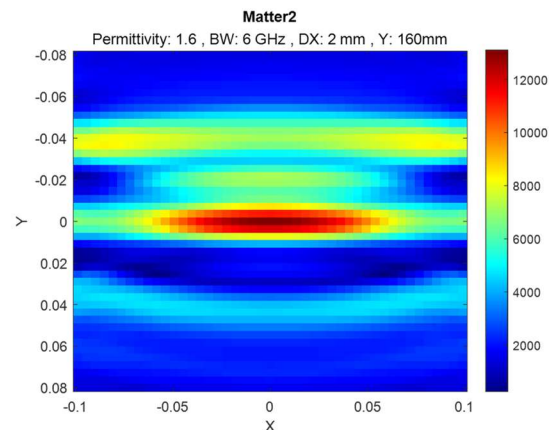

Figure 13. Shifted Matter Object

Figure 14. Shifted Matter with 1.6 Permittivity

This shifted object reconstruction was seen to be unsuccessful in targeting the shifted object change. It was noted that in all the resulting scans there was more noise in the negative Y dimension overall than before, but nothing showing true accuracy.

Next a large empty metal water bottle was scanned at the origin of the Y axis, similar to the Peanut Butter scans. The water bottle was empty because the EM waves don't respond to water located inside of the bottle. The Setup and resulting highest accuracy reconstruction shown below in *Figures 15 and 16.* The diameter of the water bottle was measured to be 9cm.
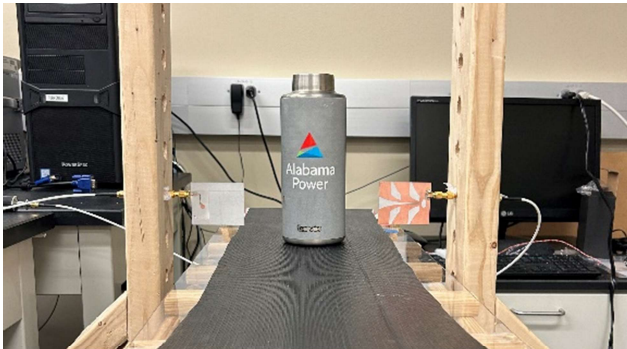

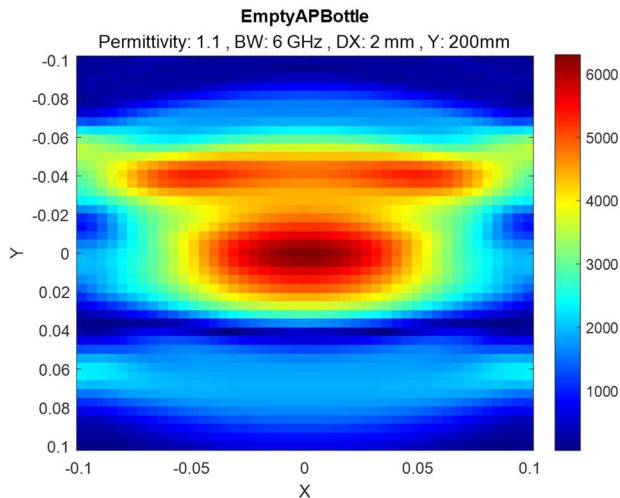
Figure 15. Metal Bottle

Figure 16. Metal Bottle DAS Reconstruction

Going any higher than a Permittivity value of 1.1 results in the negative Y dimension gaining too much noise. Similar to the case of the Peanut Butter, the X dimension of the water bottle seems to be accurate. The Y dimension, while thicker than that of the cylinder of Matter, still is inaccurate. These trends are likely due to the fact that metal has a theoretical relative permittivity of infinity. A plastic water bottle would be a better option for this MWI setup.

Next, the study of detecting the locations of a small aluminum shard inside the jar of peanut butter were conducted. These were chosen because the aluminum shard should give off a high dielectric contrast with the rest of the

peanut butter. Also, due to the peanut butter's physical characteristics, it is able to hold the aluminum shard in place in various locations and keep it still for the scanning process. This is important for testing different axis locations of the impurity within the Peanut Butter. An image of the shard is shown below in *Figure 17* being compared to the Peanut Butter, the height of the shard is 6cm while the width reaches approximately 2cm out, ending in a point. The thickness of the shard is about 1mm. The shard will first be placed in the Peanut Butter as shown, vertically and with the most surface area facing the antennas to give the highest response.

Figure 17. Aluminum Shard next to PB

The first location the shard was placed in is 2cm in the negative Y dimension, reaching from 0-2cm in the negative X direction from the center of the Peanut Butter. The actual image and a figure showing the expected location is shown in *Figure 18.*
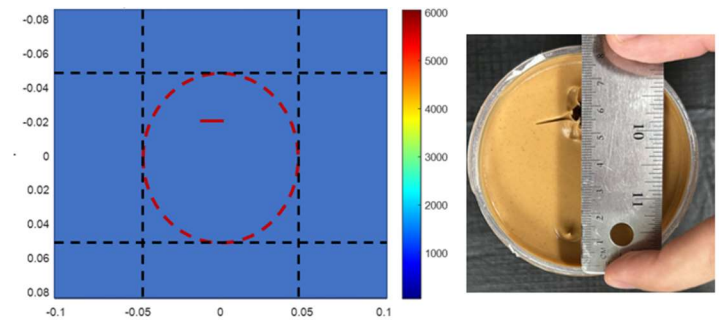

Figure 18. Impurity Location

The resulting image construction using DAS is shown in *Figure 19.* The Y dimension accuracy is spot on, however there is much symmetry in the X direction. There is also plenty of noise within the image. Using DMAS, however, we get a much more accurate result of the impurity location while drastically reducing the excess noise (*Figure 20).* Sadly, there is still symmetry over the X axis.
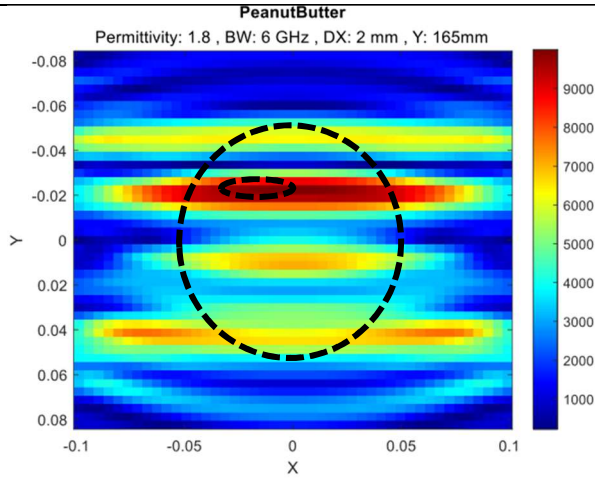
PeanutButter
Permittivity: 1.8 , BW: 6 GHz , DX: 2 mm , Y: 165mm

Figure 19. DAS Impurity Reconstruction

Figure 21. New Impurity Location +Y

PeanutButter
Permittivity: 1.8 , BW: 6 GHz , DX: 2 mm , Y: 165mm

Figure 20. DMAS Impurity Reconstruction

It can be seen that the objects Y location is accurately detected in the positive Y dimension. The highest contrast point seems to be closer to 0.02m than desired, but it is possible the jar of peanut butter was slightly skewed from the origin of the imaging domain during the scanning process, as the Antennas were mounted to a separate stand from the conveyor, and this scan was taken much later than the original impurity location scans.

PBwObj2
Permittivity: 1.5 , BW: 6 GHz , DX: 2 mm , Y: 200mm

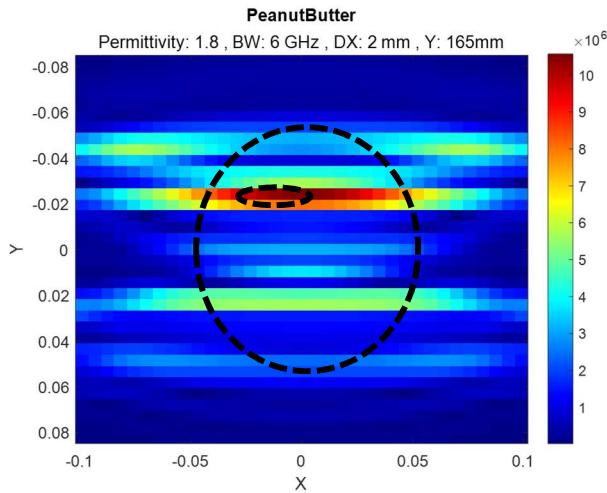Figure 22. Impurity +Y location DAS

Throughout various testing, it seems DMAS performs well with foreign object detection, rather than general object vs air reconstruction. Another scan set was taken with the object located in the same Y location but flipped over the X axis (facing the positive X direction). This resulted in a similar image, further proving the symmetry issue in the X dimension.

Next, the object was removed and placed in the positive Y direction by 3cm. It was also facing 0-2cm in the positive X direction. The image of the top of the Peanut Butter is shown below, with the general location of the impurity circled (*Figure 21*). The resulting DAS image reconstruction is also given in *Figure 22*.
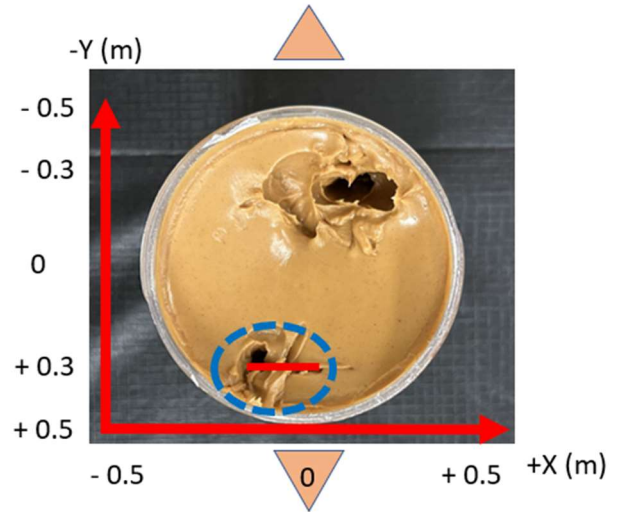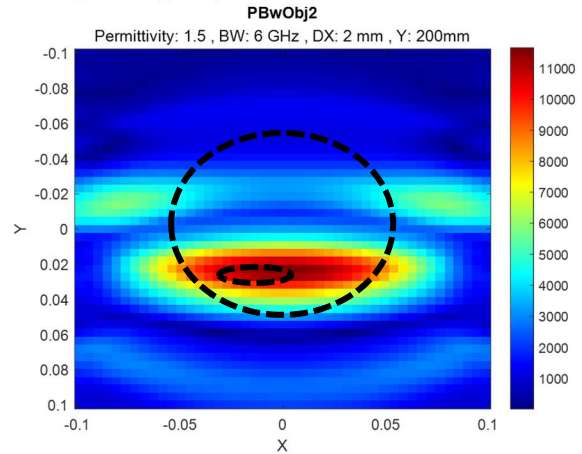
Next the Peanut Butter was rotated roughly 90 degrees counterclockwise, and then again to a total of 180 degrees, resulting with the impurity back in the negative Y direction. The following image reconstructions are shown below with *Figure 23 and 24*. It should be noted these calculations were created with an unrotated reference scan of the original Peanut Butter jar. The interior of the Peanut Butter at this point was likely not entirely uniform due to inserting and removing shards. This however shouldn't be enough to change results due to the difference in dielectric properties of aluminum and PB as well as the size of potential air pockets being so minor.
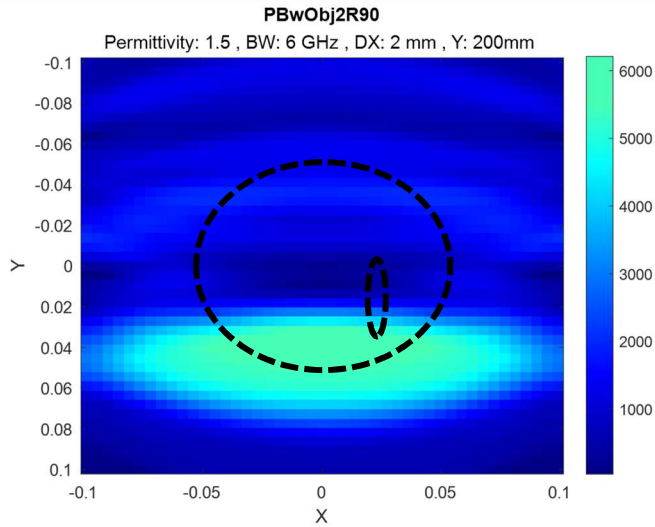
PBwObj2R90
Permittivity: 1.5 , BW: 6 GHz , DX: 2 mm , Y: 200mm

Figure 23. Impurity Rotated 90 degrees counterclockwise.

PBwObj2R180
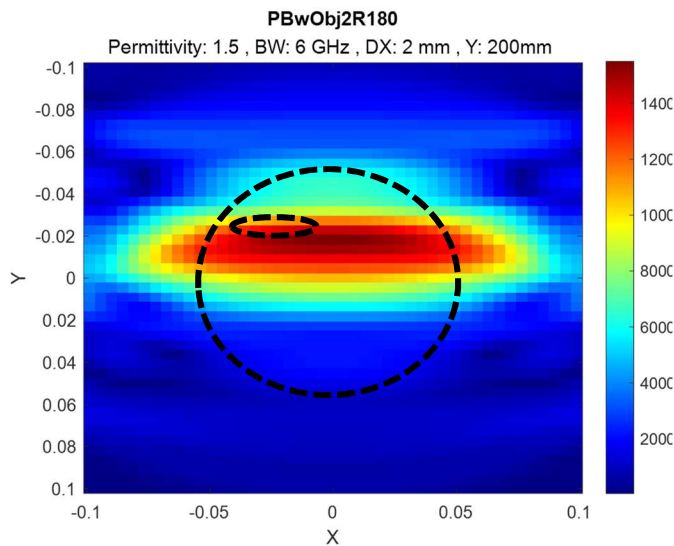Permittivity: 1.5 , BW: 6 GHz , DX: 2 mm , Y: 200mm

Figure 24. Impurity Rotate 180 degrees.

The impurity due to rotation of 90 degrees doesn't accurately show up in response to its expected location when using the same permittivity. This reconstruction's colorbar was also adjusted to match *Figure 22*'s as its average response was almost half of the unrotated version. This could be due to the fact that the shard is now parallel to the antennas and doesn't have the same wave reflection response as before. The object being rotated 180 degrees does correctly show the main response location now in the negative Y direction, but not as far in the negative Y direction as desired. The same issue that persists in all image construction issues shows up in these results. That being that there is a large amount of X dimension symmetry over the origin. This is only one set of impurity movement changing, however, and needs to be further examined.

V. CONCLUSIONS AND DISCUSSION

Throughout the testing process, it is seen that with the use of MERIT, the reconstruction of objects and impurity locations is possible, however, there is room for improvement of accuracy. It seems one of the main issues being symmetry in the X dimension, or axis of movement. It's not uncommon for images to be stretched out with the use of a Linear Antenna Array. For this use case, however, it is important to have accuracy in both directions to be able to locate foreign objects in foods. Regarding object construction, it is also important that the Y axis become more accurate in determining the varying thickness of objects.

Potential avenues of accuracy increase exist. One of these being the limiting of Bandwidth to certain parameters. The frequency response of each image construction was plotted and in some results, it's possible that limiting bandwidth in certain object and impurity cases might provide a more accurate image construction. The problem is that in other cases this might not be true and needs detailed analysis based on each individual object case.

Another potential solution to increase accuracy involves the use of Monostatic Data integration. This being the use of S11 and S22 data in the wave data gathered by the VNA. In the application of MWI of food objects discussed previously, success was found by combining Monostatic data with Bistatic data in order to reduce symmetry [1]. This was touched on during experimentation as MERIT is compatible with both bistatic and monostatic data. It was determined, however, that this would need a more detailed look than time was allotted for. This is because the way MERIT calculates delays of wave propagation would need to be different for the use of monostatic data, as the reflections of the EM waves back to the respective antennas have different propagation times than those transmitted between antennas. It is possible that combining the monostatic and bistatic data needs to be done before beamforming.

Overall, this format of imaging inline foodstuffs is definitely a potential avenue for foreign body detection. Once refined, it will form a fast, easily adjustable, and cost-effective solution to the well-known issue within the food industry.

REFERENCES

[1] J. A. Tobon Vasquez *et al.*, "Noninvasive Inline Food Inspection via Microwave Imaging Technology: An Application Example in the Food Industry," in *IEEE Antennas and Propagation Magazine*, vol. 62, no. 5, pp. 18-32, Oct. 2020, doi: 10.1109/MAP.2020.3012898.

[2] Joe Garvin, Feras Abushakra, Zachary Choffin, Bayley Shiver, Yu Gan, Lingyan Kong, Nathan Jeong, Microwave imaging for watermelon maturity determination, Current Research in Food Science, Volume 6, 2023, 100412, ISSN 2665-9271, https://doi.org/10.1016/j.crfs.2022.100412.

[3] D. O'Loughlin, M. A. Elahi, E. Porter, et al., "Open-source Software for Microwave Radar-based Image Reconstruction", Proceedings of the 12th European Conference on Antennas and Propagation (EuCAP), London, the UK, 9-13 April.

[4] M. Klemm, I. J. Craddock, J. A. Leendertz, A. Preece, R. Benjamin, "Improved Delay-and-Sum Beamforming Algorithm for Breast Cancer Detection", *International Journal of Antennas and Propagation*, vol. 2008, Article ID 761402, 9 pages, 2008. https://doi.org/10.1155/2008/761402

[5] Hooi Been Lim, Nguyen Thi Tuyet Nhung, Er-Ping Li, et al., "Confocal Microwave Imaging for Breast Cancer Detection: Delay-Multiply-and Sum Image Reconstruction Algorithm," IEEE Transactions on Biomedical Engineering, vol. 55, no. 6, pp. 1697-1704, Jun. 2008.

[6] M. Klemm, J. A. Leendertz, D. Gibbins, et al., "Microwave Radar-Based Breast Cancer Detection: Imaging in Inhomogeneous Breast Phantoms," IEEE Antennas and Wireless Propagation Letters, vol. 8, pp. 1349-1352, 2009.